Free vibration of higher-order sandwich and composite arches, Part II: Frequency spectra analysis

Sudhakar R. Marur[a,] , Tarun Kant[b]

[a]CSS Foundation, 313, A4 Wing, Cauvery Block, NGH Complex, Koramangala, Bangalore 560047, India
[b]Department of Civil Engineering, Indian Institute of Technology, Powai, Mumbai 400076, India

Abstract

The frequency spectra of the higher-order model, for laminated arches, are identified through a novel process, proposed in this paper. Besides the basic spectra corresponding to axial, flexural and shear, presence of higher-order spectra is established. Coupled spectra of first-order and higher-order degrees of freedom, in various combinations, are identified. Based on this spectra identification framework, the frequencies of sandwich and composite arches, for various boundary conditions are classified and presented. Also, the role of curvature and aspect ratio on the fundamental frequency of arches with various end-conditions is investigated, in the second part of this paper.

1. Introduction

In most of the free vibration-related formulations, the main focus would be to extract few fundamental frequencies and benchmark the same with results obtained through either experimental or computational or analytical means. The order of effort towards the exploration of Eigenvectors, the true and large repository of information into the modes of vibration, is rather much less compared to that of eigenvalues. However, there are quite a few works, which investigate deeper into the modes and frequency spectrums. Wolf [1] studied the free vibrations of elastic circular arches through a direct iterative eigensolution method. He computed the energy distribution of each mode and quantitatively assessed the nature of frequency spectrum, for various slenderness ratios. Veletsos et al. [2] studied the free in-plane vibration of circular arches. They classified the modes, based on the modal patterns and associated strain energies, as purely flexural, purely extensional and breathing modes (wherein flexural and axial are coupled). Also, the conditions under which each one of these modes would be operative had been defined and simple formulae to predict the same have been derived. Austin and Veletsos [3] extended the study of Veletsos et al. [2], by incorporating rotatory inertia and shear deformation into the formulation. They classified the modes as entirely inextensional (with flexural and shearing coupled), primarily extensional (with negligible shear and rotatory inertia effects) and coupled modes (as mixture of above two modes).

Bhashyam and Prathap [4] detected the second spectrum of frequencies, known as shear mode, in addition to the first spectrum or flexural mode for the beam problems using isoparametric linear elements. Heppler [5] employed Timoshenko beam finite elements, using trigonometric basis functions for the free-vibration studies of arches, wherein he had extracted the rigid body modes and other elastic modes for various subtended angles of 60°, 180° and 360°. Sakiyama et al. [6] studied the vibration characteristics of sandwich arches with elastic and visco-elastic core, with the identification of axial and flexural modes. Prathap and Vinayak [7] studied the vibration problem of higher-order composite beams, by clearly identifying the basic modes vibrations, i.e. axial, flexural and shear for various lay up sequences and boundary conditions. Also, they established that for single layer and symmetric multi-layer configurations these basic modes do not couple amongst themselves while for non-symmetric lay-ups, their coupling effect seem to be more prevalent. Blevins [8] presented in greater detail, an exhaustive list of formulae for computing the natural frequencies and corresponding mode shapes of various structures. Using Timoshenko's first-order shear theory (FOST) [9,10] based two noded curved beam element, Jafarali et al. [11] studied the free vibrations of deep arches and extracted three basic spectrums—axial, flexural and shear. Marur and Kant [15,16] analyzed the composite and sandwich beams, using higher-order theory and classified the resulting frequencies into similar basic three spectrums and compared them with those from FOST (Table 1).

As one can see, besides the three basic spectra such as axial, flexural and shear, there are coupled spectrums even in isotropic cases and more so in composite materials. In the case of arches, that are thicker and deeper with composite and sandwich material constructions, it becomes important to adopt the higher-order model [17] and explore the pure spectrums of higher-order degrees of freedom (dof) and the coupled spectrums of basic dof and higher-order dof, to understand the vibration behavior of such structures.

In order to achieve that, a frequency spectrum identification process is proposed in this paper, using which, the pure and coupled spectrums are clearly captured. Besides the spectrums corresponding to basic or first-order dof, pure spectrums corresponding to higher-order dof are also identified. In the case of coupled spectrums, their existence in various combinations such as twin dof, triple dof, quadruple dof and even quintuple dof is established. Based on this spectrum identification framework, frequencies of thick, symmetric and un-symmetric, sandwich and composite arches for various end-conditions are classified and tabulated. Subsequently, the role of curvature and aspect ratios on the fundamental frequency of symmetric sandwich and un-symmetric composite arches with various boundary conditions is studied and suitable conclusions are drawn.

2. Frequency spectra identification process

The real nature of an eigenvalue or frequency can be ascertained only through a systematic study of its eigenvector, representing the corresponding mode shape. However, the eigenvector extracted through an eigenvalue solver, cannot be employed directly to study the frequency spectrum. The elements of eigenvector corresponding to each eigenvalue need to be made dimensionally consistent first and normalized later, for the identification and meaningful study of spectrums. A frequency spectrum identification process proposed in this section, is as follows:

- The eigenvector is first extracted for each frequency, from the solver.
- The elements of this vector correspond to the seven dof—u_0, w_0, θ_x, u_0*, θ_0*, θ_z, w_0*—for every node, from 1 to *nn*, as in the higher-order displacement model

$$u = u_0 + z\theta_x + z^2 u_0^* + z^3 \theta_x^*, \tag{1}$$

$$w = w_0 + z\theta_z + z^2 w_0^*, \tag{2}$$

where z is the distance from the neutral axis to any point of interest along the depth of the arch, u_0 and w_0 are axial and transverse displacements in x–z plane, θ_x is the face rotation about y-axis and u_0*, θ_x*, θ_z,w_0* are the higher-order terms arising out of Taylor's series expansion and defined at the neutral axis and *nn* represents the total number of nodes, in the arch model.

Table 1
Data for numerical experiments

1.1. Nomenclature
FOST—first-order shear deformation theory [9]
k—shear correction factor for FOST [10]
S—arc length of the arch
t—thickness of cross section
R—radius of curvature
S/t—aspect ratio
β ($= S/R$)—subtended angle of an arch
FNP—frequency normalizing parameter
BC—boundary condition

1.2 Boundary conditions for different supports

Support type	At $x=0$	At $x=S$
Simply supported (SS)	$u_0 = u_0^* = 0$ $w_0 = \theta_z = w_0^* = 0$	$u_0 = u_0^* = 0$ $w_0 = \theta_z = w_0^* = 0$
Simply support-roller (SR)	$u_0 = u_0^* = 0$ $w_0 = \theta_z = w_0^* = 0$	$w_0 = \theta_z = w_0^* = 0$
Clamped–clamped (CC)	$u_0 = u_0^* = \theta_x = \theta_x^* = 0$ $w_0 = \theta_z = w_0^* = 0$	$u_0 = u_0^* = \theta_x = \theta_x^* = 0$ $w_0 = \theta_z = w_0^* = 0$
Clamped-free (CF)	$u_0 = u_0^* = \theta_x = \theta_x^* = 0$ $w_0 = \theta_z = w_0^* = 0$	All free

1.3. Material data

No.	Details	Ref.
Data-1		
	$E_1 = E_2 = E_3 = 2 \times 10^5$	[11]
	$G_{12} = G_{23} = G_{13} = 10^5$	
	$v = 0,\ \rho = 1,\ b = 10,\ t = 50$	
	$R = 1273.2,\ S = 1000$	
	$\beta = 45^\circ$	
	k (for FOST) $= 1.2$	[10]
	FNP : $S^2\sqrt{\dfrac{12\rho}{E_1 t^2}}$	
	No. of elements: 15 cubic	
	BC: SR	
Data-2		
	$S = 30\,\text{in},\ b = 1\,\text{in}$	
	$S/t = 5,\ S/R = \pi/2$	
	Face: graphite/epoxy	[12]
	t_f (top, bot.) $= 0.6\,\text{in}$	
	$E_x = 0.1742 \times 10^8$ psi	
	$E_y = E_z = 0.1147 \times 10^7$ psi	
	$G_{xy} = G_{yz} = G_{xz} = 0.7983 \times 10^6$ psi	
	$\rho = 0.1433 \times 10^{-3}\,\text{lb}\,\text{s}^2/\text{in}^4$	
	$v = 0.3$	
	Core: Aluminium honeycomb (0.25 in cell size, 0.007 in foil)	[13]
	$t_c = 4.8\,\text{in}$	
	$E_x = E_y = E_z = G_{xy} = 0$	
	$G_{yz} = 0.1021 \times 10^5$ psi	
	$G_{xz} = 0.2042 \times 10^5$ psi	
	$\rho = 0.3098 \times 10^{-5}\,\text{lb}\,\text{s}^2/\text{in}^4$	
	$t_c/t_f = 8$	

Table 1 (*continued*)

	Lamination scheme: 0/30/45/60/core/60/45/30/0	
	FNP : $S^2\sqrt{\dfrac{12\rho_f}{E_{fx}t^2}}$	
	No. of elements: 15 cubic	
Data-2a	BC: SS with Data-2	
Data-2b	BC: CC with Data-2	
Data-2c	BC: CF with Data-2	
Data-3		
	Lamination scheme: 0/90/core/0/90	
	Rest are same as Data-2	
Data-3a	BC: SS with Data-3	
Data-3b	BC: CC with Data-3	
Data-3c	BC: CF with Data-3	
Data-4		[14]
	$S = 30\,\text{in},\ S/R = \pi/2$	
	$E_x = 0.762 \times 10^8\,\text{psi}$	
	$E_y = E_z = 0.3048 \times 10^7\,\text{psi}$	
	$G_{xy} = G_{yz} = G_{xz} = 0.1524 \times 10^7\,\text{psi}$	
	$v = 0.25,\ \rho = 0.72567 \times 10^{-4}\,\text{lb s}^2/\text{in}^4$	
	$b = 1\,\text{in},\ t = 6\,\text{in}$	
	Lamination scheme: 30/–30/30	
	FNP : $S^2\sqrt{\dfrac{12\rho}{E_1t^2}}$	
	No. of elements: 15 cubic	
Data-4a	BC: SS with Data-4	
Data-4b	BC: CC with Data-4	
Data-4c	BC: CF with Data-4	
Data-5		[14]
	$S = 30\,\text{in},\ S/R = \pi/2$	
	$E_x = 0.762 \times 10^8\,\text{psi}$	
	$E_y = E_z = 0.3048 \times 10^7\,\text{psi}$	
	$G_{xy} = G_{yz} = G_{xz} = 0.1524 \times 10^7\,\text{psi}$	
	$v = 0.25,\ \rho = 0.72567 \times 10^{-4}\,\text{lb s}^2/\text{in}^4$	
	$b = 1\,\text{in},\ t = 6\,\text{in}$	
	FNP : $S^2\sqrt{\dfrac{12\rho}{E_1t^2}}$	
	No. of elements: 15 cubic	
	BC: SS	
Data-5a	Lamination scheme: 0 with Data-5	
Data-5b	Lamination scheme: 90 with Data-5	
Data-5c	Lamination scheme: 0/90 with Data-5	
Data-5d	Lamination scheme: 90/0 with Data-5	
Data-6		
	Lamination scheme: 0/45/–45/90	
	Rest are same as Data-4	
Data-6a	BC: SS with Data-6	
Data-6b	BC: CC with Data-6	
Data-6c	BC: CF with Data-6	

- All Eigenvector elements corresponding to θ_x, u_0*, θ_x*, θ_z and w_0* are to be multiplied by z and its powers, as in Eqs. (1) and (2), to make all of them dimensionally consistent while those corresponding to u_0 and w_0 can be retained as such, as these two dimensionally represent displacement terms.
- Elements of eigenvector corresponding to θ_x and θ_z are multiplied by $(t/2)$, u_0* and w_0* by $(t/2)^2$ and θ_x* by $(t/2)^3$, where $(t/2)$ represents half of the cross sectional thickness of the arch. This value of $(t/2)$ is taken for z, in order to consider the maximum displacement, at the top of the cross section.

- Now, all elements of the eigenvector become displacement terms, from the dimensional stand point.
- The highest element of the eigenvector is then identified.
- The whole vector is divided by this highest element, which transforms it into a normalized eigenvector.
- The elements corresponding to u_0 of all the nodes (1 to *nn*), from the normalized eigenvector, are collected and plotted. Similarly, elements corresponding to other dof are also collected and plotted on the same graph. This generates the frequency spectrum plot for a given eigenvalue or frequency. As all the values are dimensionally displacements, which are normalized between -1 and 1, they can be directly compared and contrasted, to classify a frequency into a specific spectrum.
- *Pure spectrums*: In a frequency spectrum plot, if the elements of a normalized eigenvector, corresponding to any one dof reach the peak value of -1 (as u_0* in Fig. 5a) or $+1$ (as w_0 in Fig. 1a) or both (as θ_z in Fig. 5c), on the y-axis—*known as the dominant dof*—while the elements of all other dof are less than $+0.5$ or greater than -0.5, then it forms the pure spectrum of that dominant dof. Examples of various pure modes are shown in Figs. 1–5.
- *Coupled spectrums*: In a frequency spectrum plot, if the elements of a normalized eigenvector, corresponding to any one dof reach the peak value of $+1$ (as w_0 in Fig. 6b) or -1 (as θ_x in Fig. 6d) or both (as w_0 in Fig. 6a), on the y-axis, with the elements of some more dof exceeding the -0.5 (as u_0 in Fig. 6a) or $+0.5$ mark (as u_0* in Fig. 10d) or both (as w_0 in Fig. 8f)—*known together as dominant dofs*—then it forms the coupled spectrum of those dominant dofs. Examples of various coupled modes are shown in Figs. 6–11.

3. Frequency spectra of higher-order model

3.1. Pure first-order spectrums

The frequency spectrums corresponding to the physical dof, i.e. u_0, w_0, θ_x—axial, flexural and shear modes of a beam are very well studied and established [4,7]. These three spectrums for a thin circular arch (Table 2) are presented in Figs. 1–3, wherein the close agreement of frequencies and spectrums of current formulation with those of Ref. [11] can be observed. Subsequently, the pure first-order spectrums of a deep arch are presented in Fig. 4.

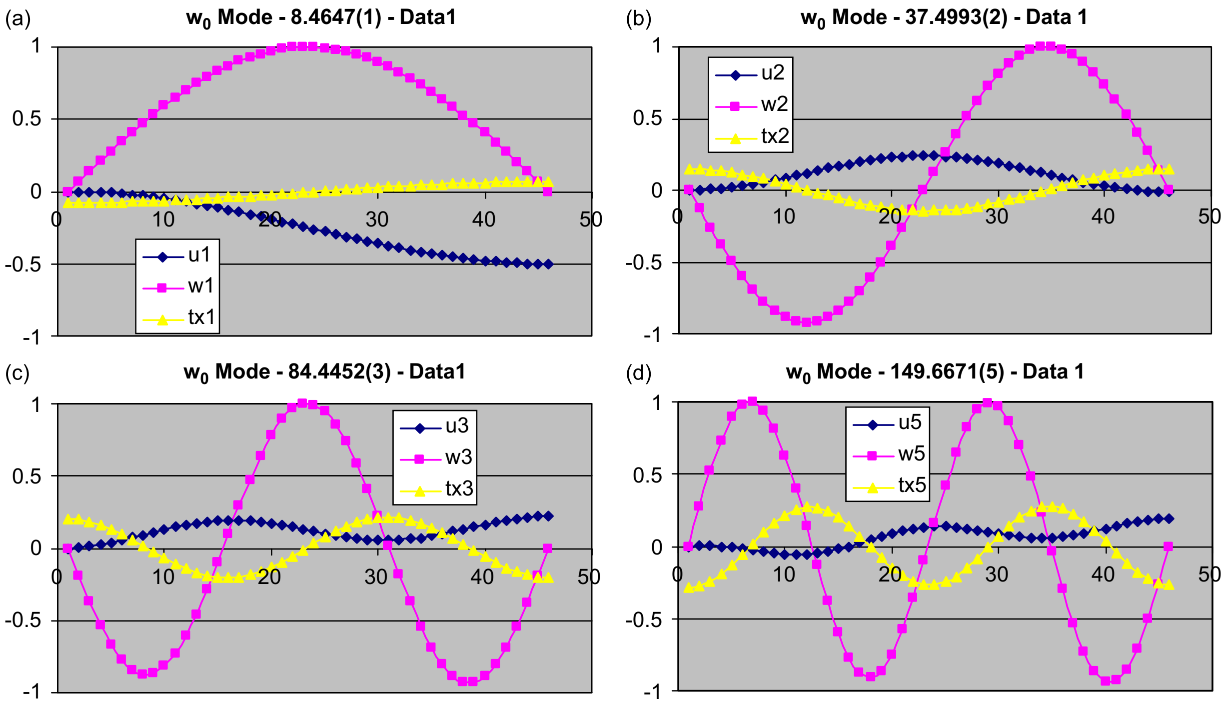

Fig. 1. (a)–(d) Flexural spectrum of thin circular arch.

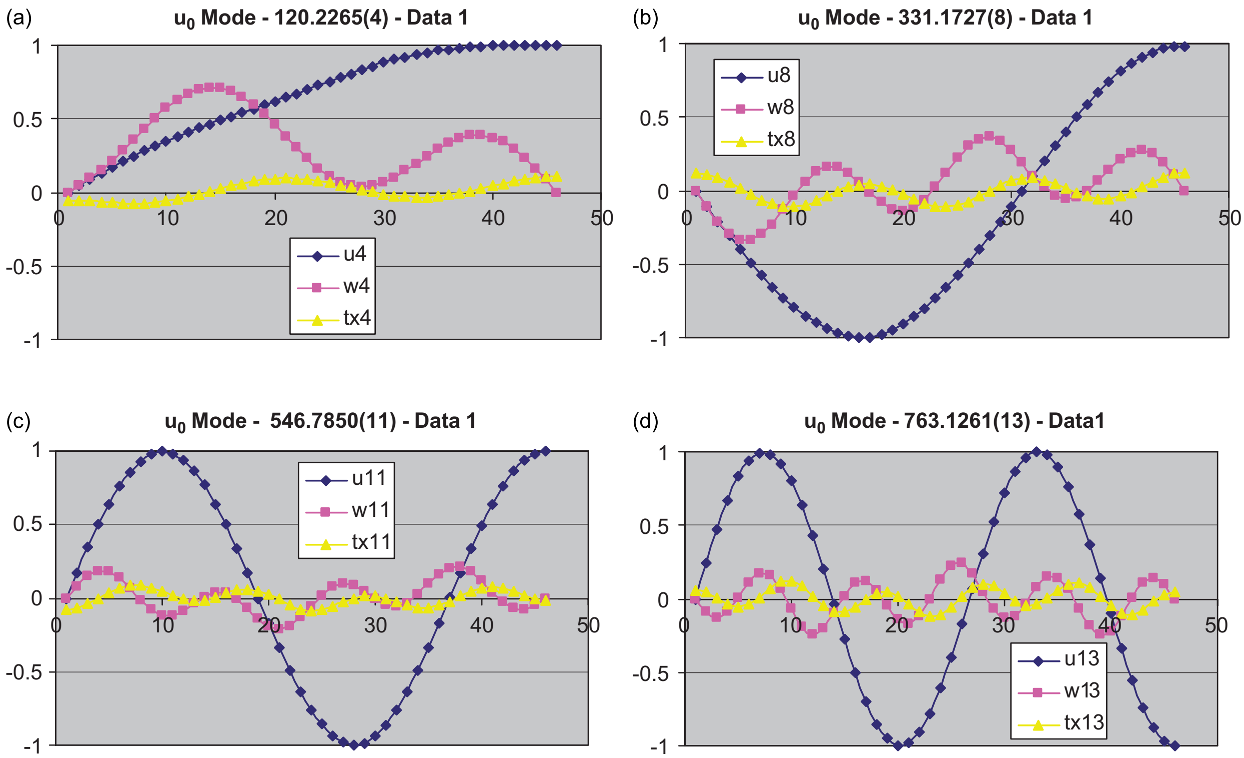

Fig. 2. (a)–(d) Axial spectrum of thin circular arch.

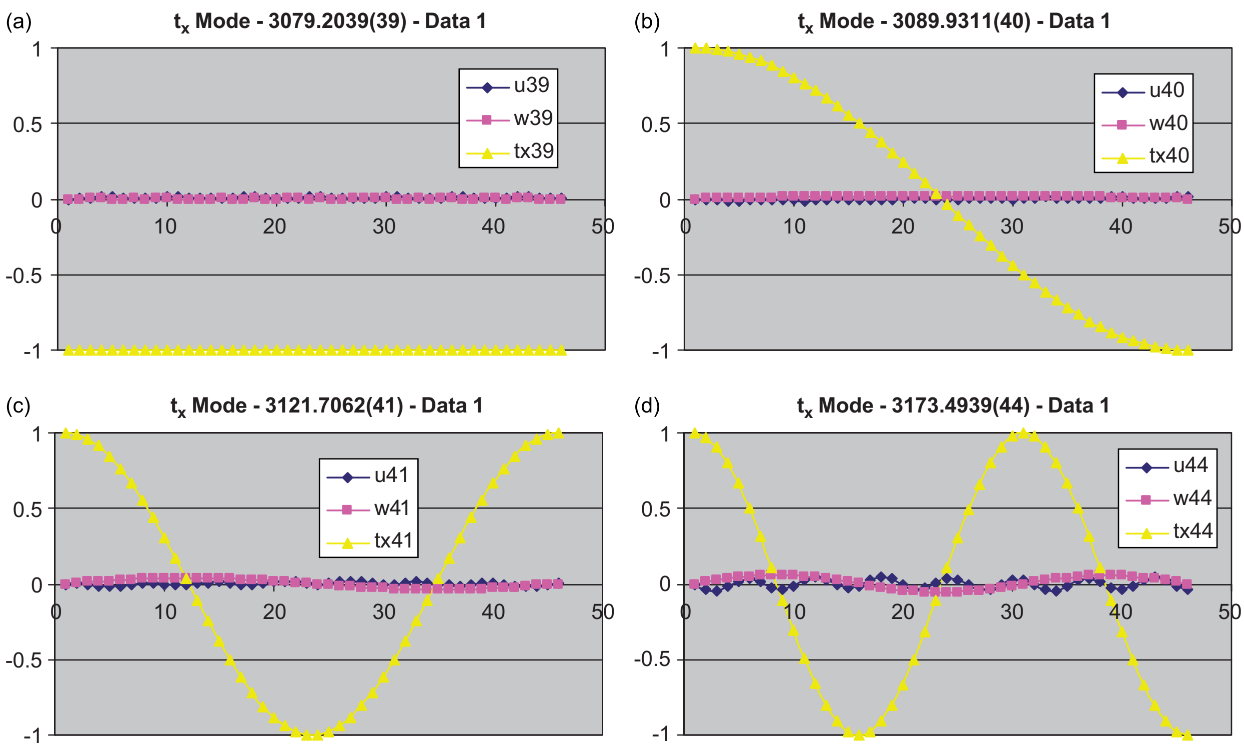

Fig. 3. (a)–(d) Shear spectrum of thin circular arch.

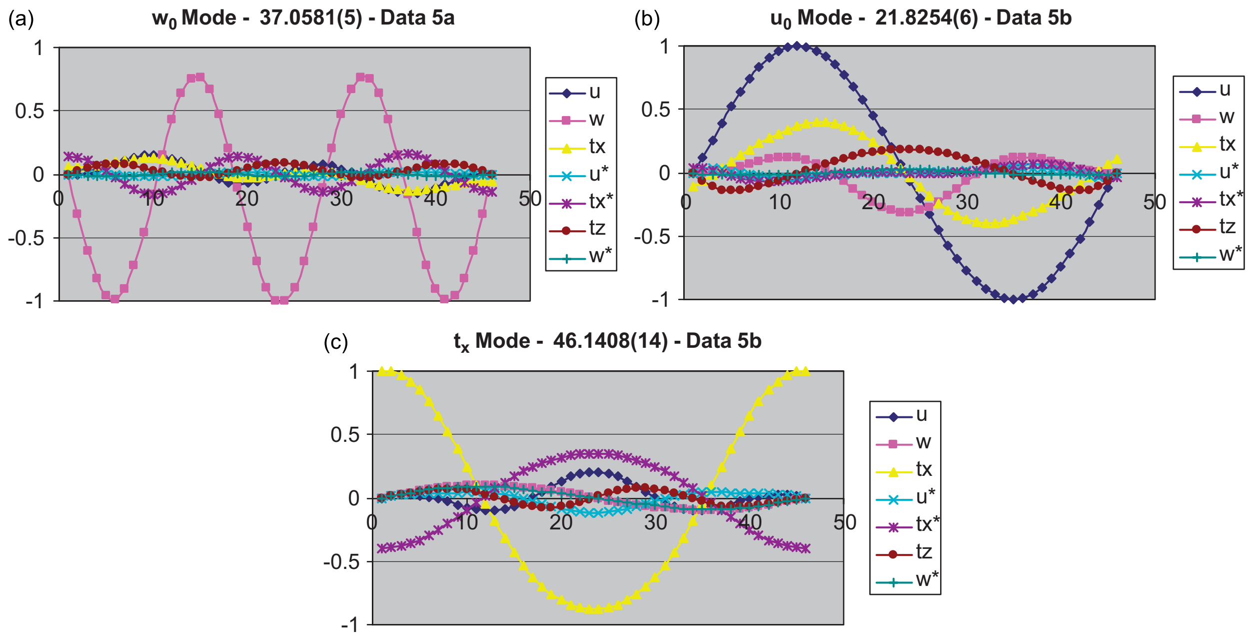

Fig. 4. (a)–(c) Flexural, axial and shear spectrums of thick circular arch.

3.2. *Pure higher-order spectrums*

As the cross section becomes thicker or aspect ratio becomes smaller, higher-order spectrums, corresponding to higher-order dof become active. These pure spectrums corresponding to u_0*, θ_x*, θ_z, w_0* are captured in Fig. 5a–h.

3.3. *Coupled spectrums*

Whenever the elements of two dof, of a normalized eigenvector, are dominant, then it is known as twin dof coupled spectrum. Similarly, one can observe the existence of triple, quadruple as well as quintuple dof coupled spectrums, in the case of deep composite and sandwich arch vibration problems.

3.3.1. *Twin dof coupled spectrum*

This spectrum may have two dominant dofs—either two first order or two higher order or a first and higher order.

3.3.1.1. FO–FO coupling. The spectrum with two first-order dof (FO–FO) being dominant are shown in Fig. 6a and b (u_0–w_0), c (u_0–θ_x) and d (w_0–θ_x).

3.3.1.2. HO–HO coupling. The spectrum with two higher-order dof (HO–HO) being dominant is shown in Fig. 7a (u_0*–θ_x*), b (u_0*–θ_z), c (u_0*–w_0*), d (θ_x*–w_0*) and e (θ_z–w_0*).

3.3.1.3. FO–HO coupling. The spectrum with one first order and one higher-order dof (FO–HO) being dominant is shown in Fig. 8a (u_0–u_0*), b (u_0–θ_x*), c (u_0–θ_z), d (w_0–u_0*), e (w_0–θ_x*), f (w_0–θ_z), g (θ_x–u_0*), h (θ_x–θ_x*), i (θ_x–θ_z) and j (θ_x–w_0*).

3.3.2. *Triple dof coupled spectrum*

In this spectrum, any three dof could be dominant. Various combinations of dominant dof can be seen in Tables 3–14. Few examples are shown in Fig. 9a (u_0–w_0–θ_x), b (u_0–θ_x–θ_x*), c (u_0–θ_x–θ_z), d (u_0–u_0*–θ_z),

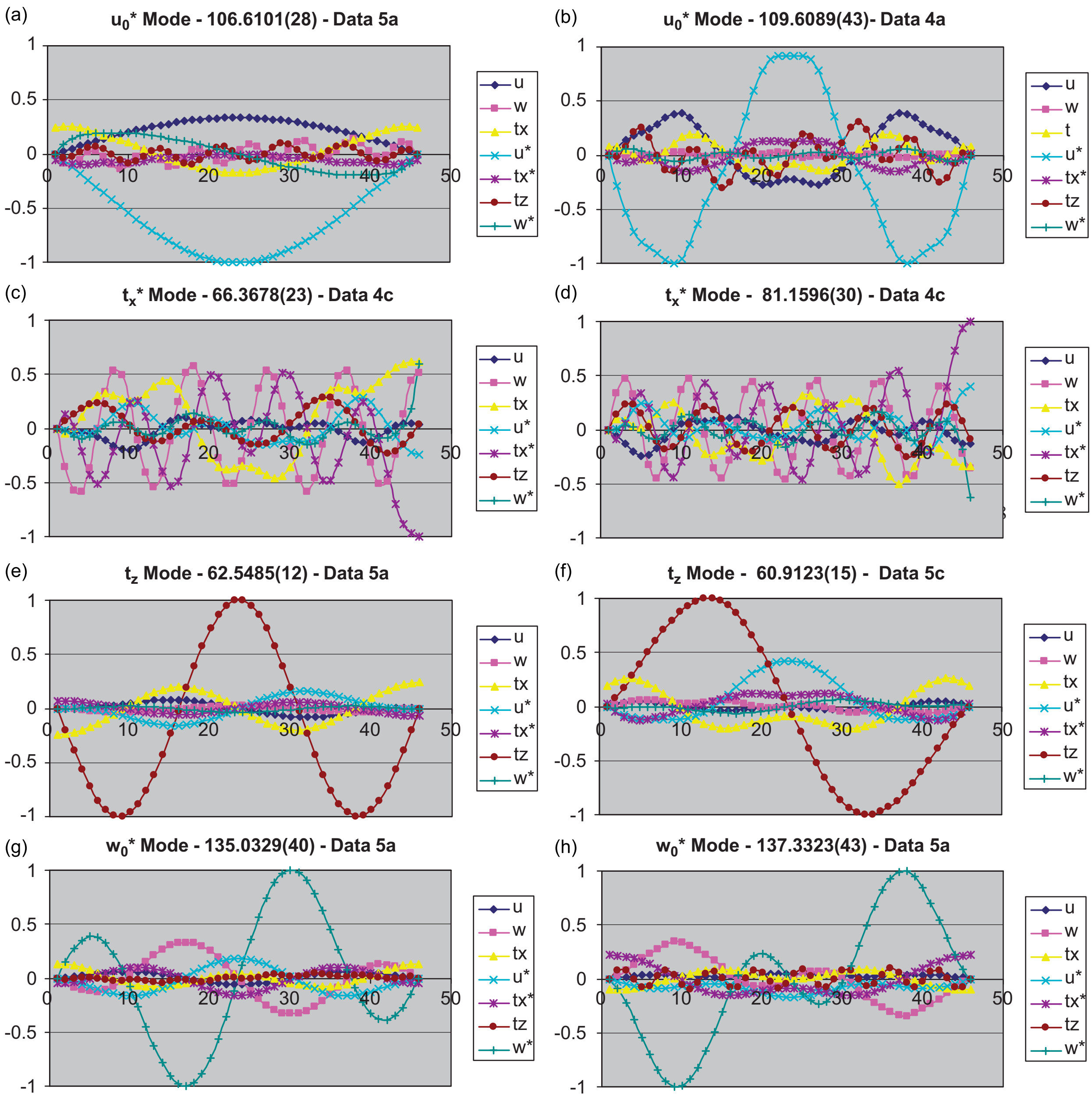

Fig. 5. (a)–(b) u_0* spectrum of thick circular arch; (c)–(d) θ_x* spectrum of thick circular arch; (e)–(f) θ_z spectrum of thick circular arch; (g)–(h) w_0* spectrum of thick circular arch.

e (w_0–θ_x–θ_x*), f (w_0–u_0*–θ_x*), g (w_0–u_0*–θ_z), h (w_0–θ_x*–θ_z), i (θ_x–u_0*–θ_z), 9j (θ_x–θ_x*–w_0*), k and l (u_0*–θ_x*–θ_z).

3.3.3. *Quadruple dof coupled spectrum*

The spectrum with four dof being dominant can be seen in Tables 3–14. Also, few cases are shown in Fig. 10a (u_0–w_0–θ_x–θ_x*), b (u_0–θ_x–u_0*–θ_x*), c (w_0–u_0*–θ_x*–θ_z) and d (θ_x–u_0*–θ_x*–θ_z).

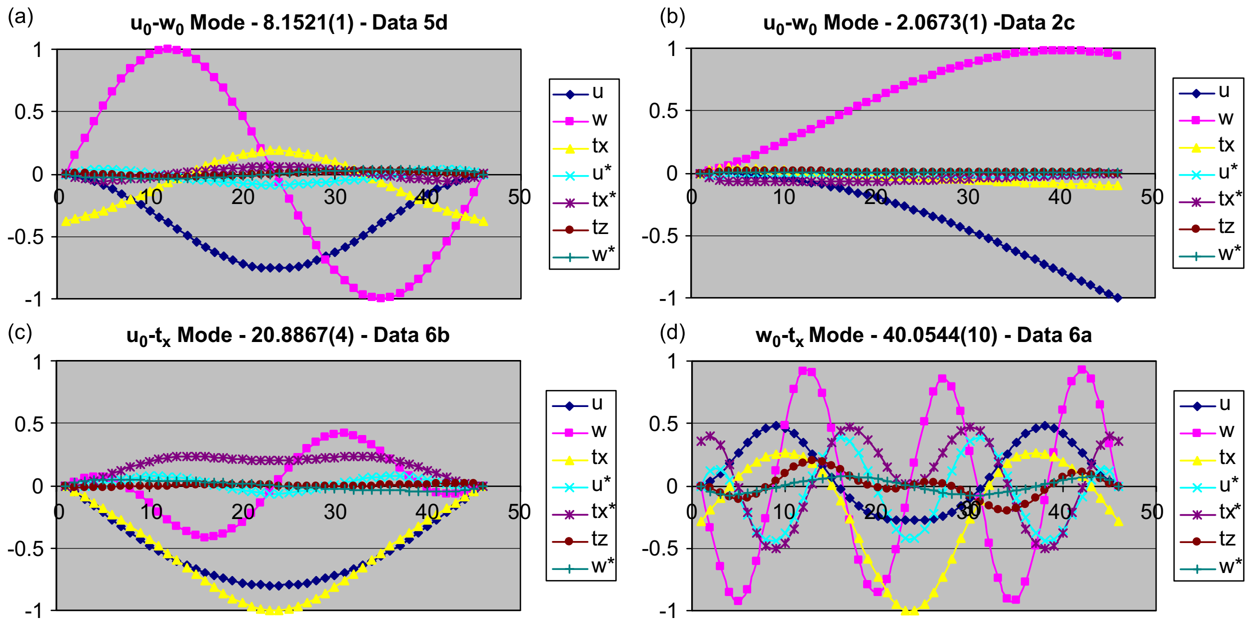

Fig. 6. (a)–(d) Twin dof coupled spectrum (FO–FO) of thick circular arch.

3.3.4. *Quintuple dof coupled spectrums*

The spectrum with five dof being dominant can be observed in Tables 3–14 as well as in Fig. 11a–c (u_0–θ_x–u_0*–θ_x*–θ_z).

4. Frequency analysis of sandwich and composite arches

Next, symmetric and unsymmetric composite and sandwich arches with an aspect ratio of five and a subtended angle of 90° are studied (Data-2–4, Data-6) for various boundary conditions. The frequencies obtained through the higher-order model are classified according to their spectrums (Tables 3–14), and the values given in parenthesis for each frequency correspond to the actual mode of arch vibration.

In the case of composite arches, one can observe more frequencies of pure and twin dof coupled spectrums. Quintuple dof coupled spectrum does not exist for this case. The highest order of coupling in symmetric and unsymmetric composites is triple dof and quadruple dof spectrums, respectively.

On the other hand, for sandwich arches, more of coupled spectrums can be observed. In the case of symmetric sandwich arches with SS end-condition, more frequencies of triple, quadruple and quintuple dof coupled spectrums can be found; for CC and CF end-conditions, frequencies of pure spectrums are quite a few.

In the case of unsymmetric sandwich arches with SS end-condition, more frequencies of triple and quadruple dof coupled spectrums exist while for CC end-condition, very few frequencies of pure spectrums can be observed. The unsymmetric sandwich arch with CF end-condition, however, demonstrates a different pattern—more frequencies of pure and twin dof coupled spectrums compared to other spectrum patterns.

Out of 21 possible combinations in twin dof coupled spectrum (three FO–FO, six HO–HO and twelve FO–HO couplings), the combination of θ_x*–θ_z from HO–HO, u_0–w_0* and w_0–w_0* from FO–HO couplings could not be observed, for any of the material set or boundary conditions in Data-2–6.

While many combinations of triple dof and quadruple dof can dominate the frequency spectrum plot, seventeen combinations of triple dof and six combinations of quadruple dof spectrums can be observed from these tables, for the given data set.

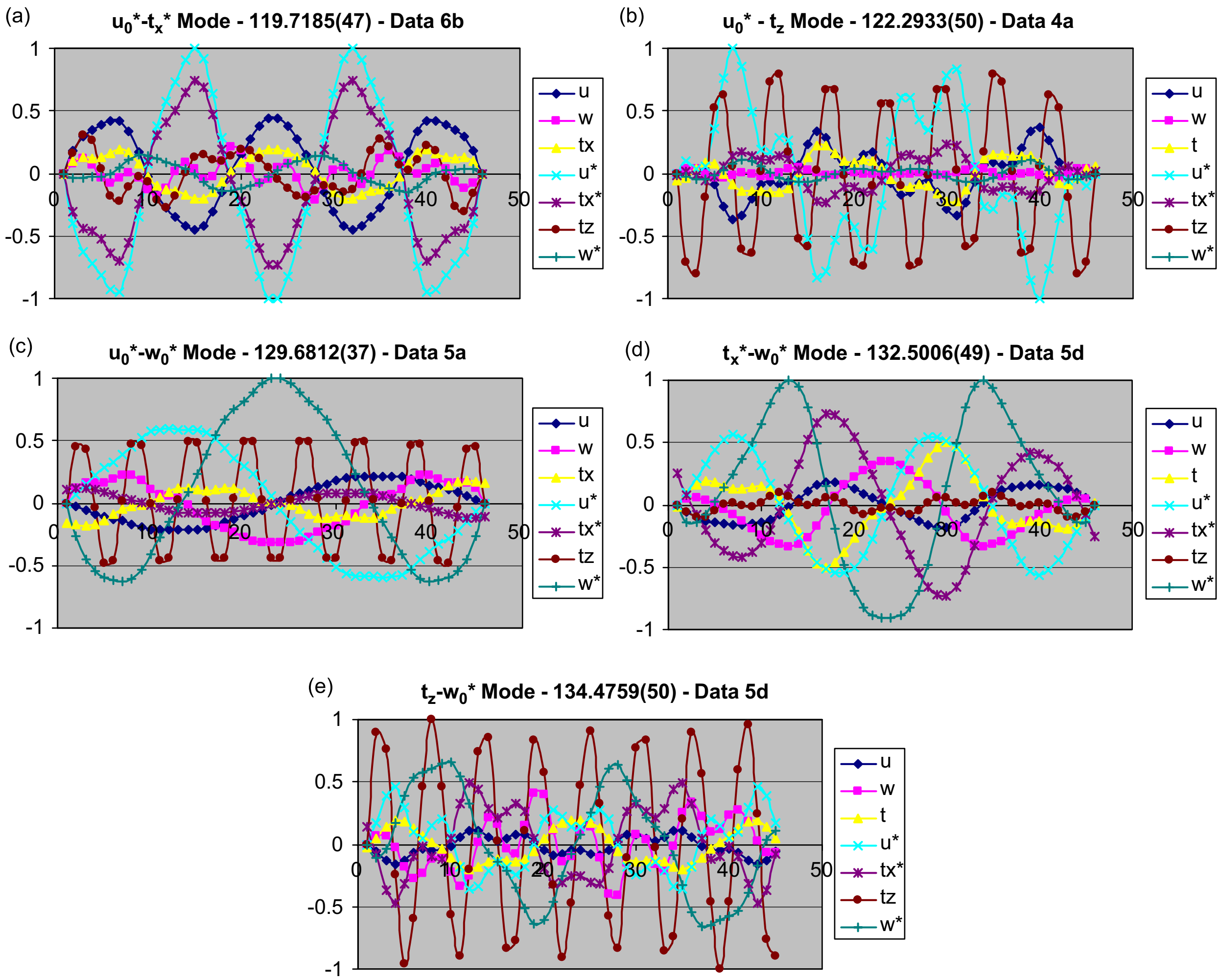

Fig. 7. (a)–(e) Twin dof coupled spectrum (HO–HO) of thick circular arch.

Similarly, in the case of quintuple dof coupled spectrum, only one unique combination of dof is seen (u_0–θ_x–u_0*–θ_x*–θ_z), for various end-conditions of sandwich arches.

5. Parametric studies

In order to study the influence of curvature, aspect ratios and boundary conditions on the fundamental frequency, parametric studies have been conducted using the symmetric sandwich (Data-2) as well as unsymmetrical composite material (Data-6). The responses from the higher-order model are captured through Figs. 12–21 and some of the key observations are as follows:

- As the curvature increases, simply supported (SS) and clamped–clamped (CC) arches become stiffer and frequencies keep increasing. At a particular curvature value, the stiff system transitions into a softer one and frequencies start decreasing thereafter.
- This transition value of curvature is dependent on aspect ratio and lay up sequence:
  - For thick sandwich arches ($S/t \leqslant 15$), the transition happens at 60°.
  - For thin sandwich arches ($S/t > 15$) at 45° or less.

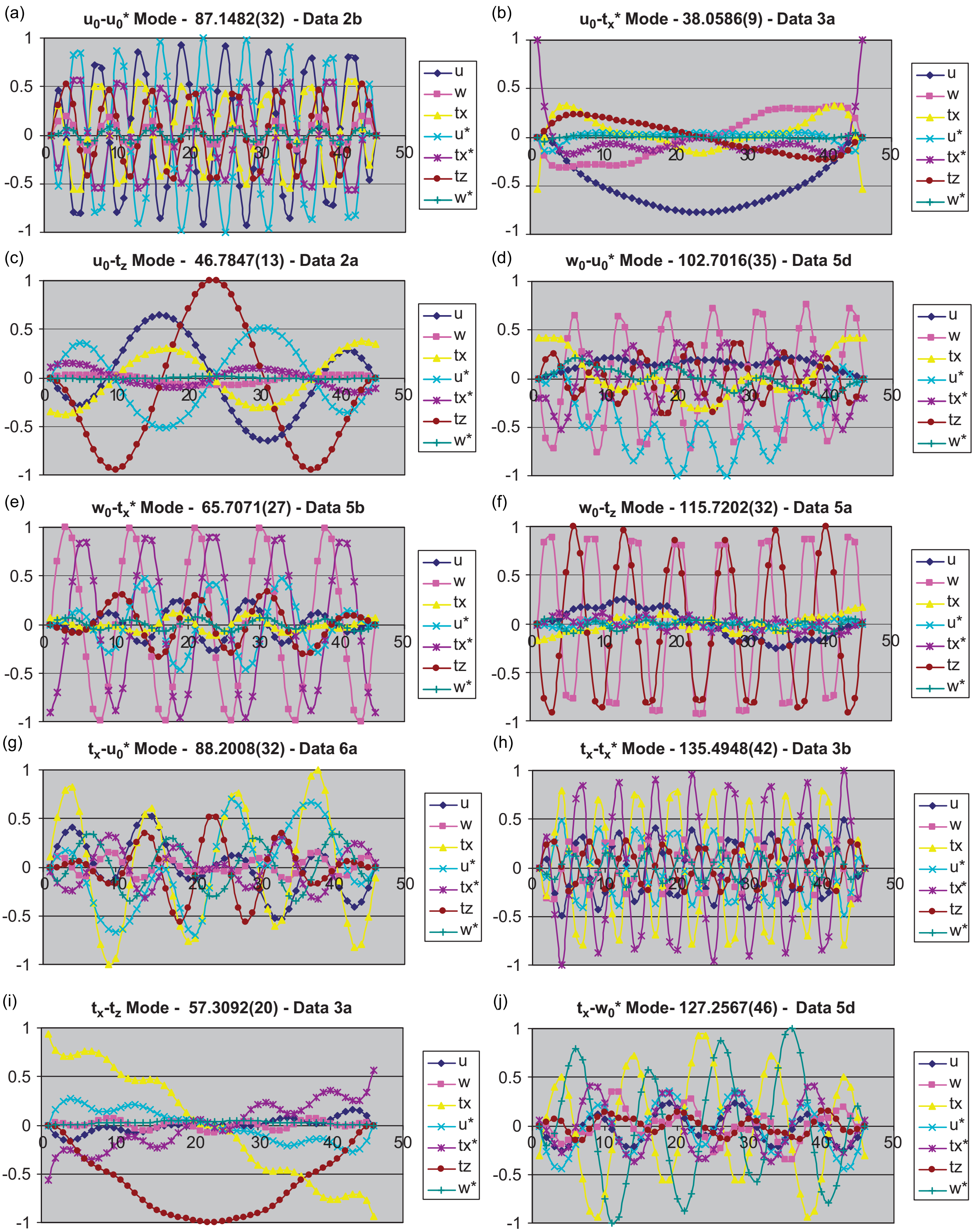

Fig. 8. (a)–(j) Twin dof coupled spectrum (HO–FO) of thick circular arch.

- ○ In the case of thick composite arches, it varies between 90° and 45°, depending on end-conditions.
- ○ For thin composite arches ($S/t > 15$), it occurs at 30°.
- The rate of softening of SS arch is much steeper than that of CC arch. However, no such transition can be observed in the case of clamped–free (CF) arches, wherein the frequencies keep increasing with the increase in curvature.
- The CC end-condition produces perhaps the stiffest system while CF end-condition makes the softest system. The system with SS end-condition falls in between these two.
- The change in aspect ratio (S/t) from low to high makes the system from being soft to stiff.

6. Conclusions

A novel spectra identification process is proposed in this paper. Besides the basic or first-order spectra corresponding to axial, flexural and shear, the existence of higher-order spectra as well as coupled spectra in various combinations of first and higher-order dof, such as twin, triple, quadruple and even quintuple are identified. Based on the spectrum identification framework, frequencies of thick, symmetric as well as unsymmetric, laminated arches for various boundary conditions are classified and tabulated. Subsequently, the role of curvature, aspect ratios and boundary conditions on the fundamental frequency are studied using the symmetric sandwich and unsymmetric composite material and suitable conclusions are drawn.

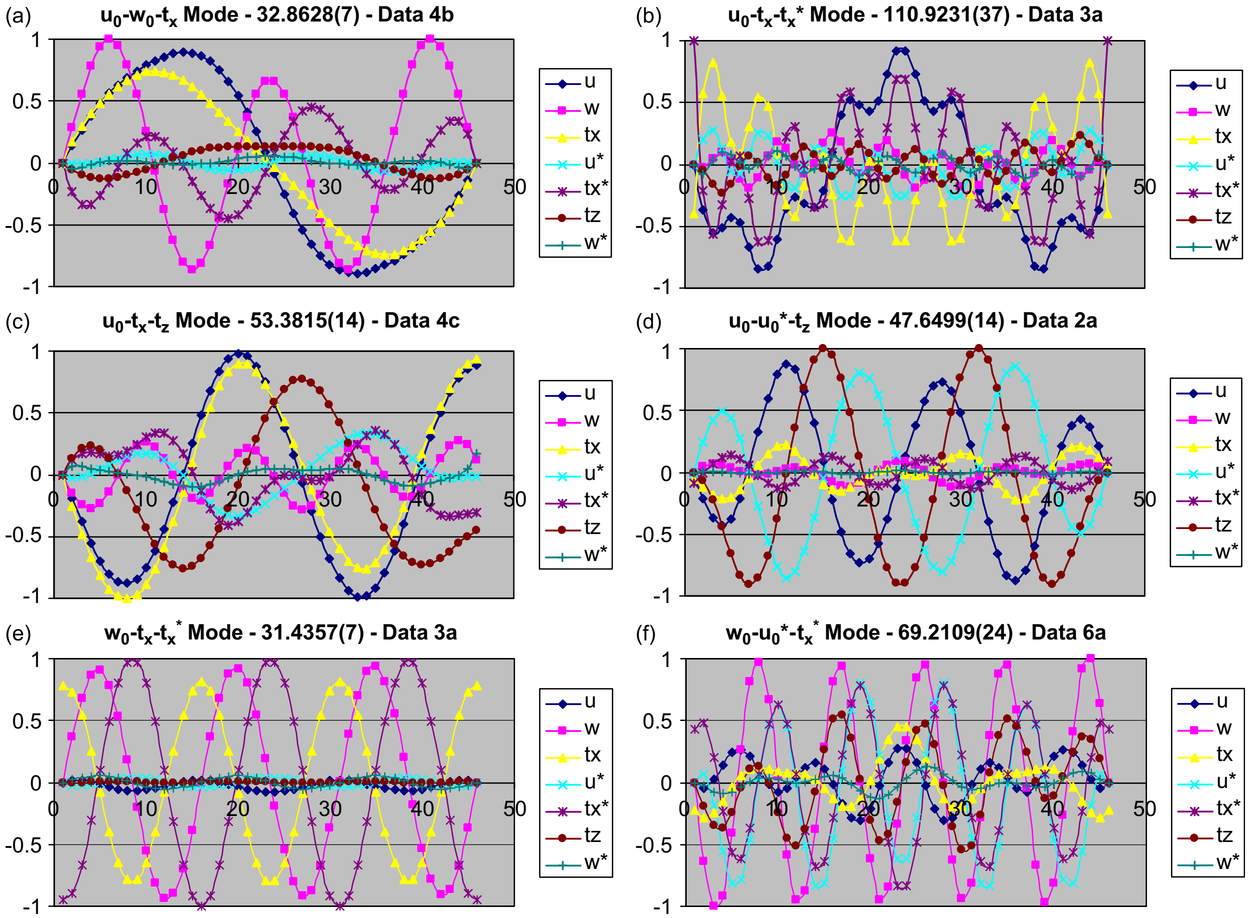

Fig. 9. (a)–(l) Triple dof coupled spectrum of thick circular arch.

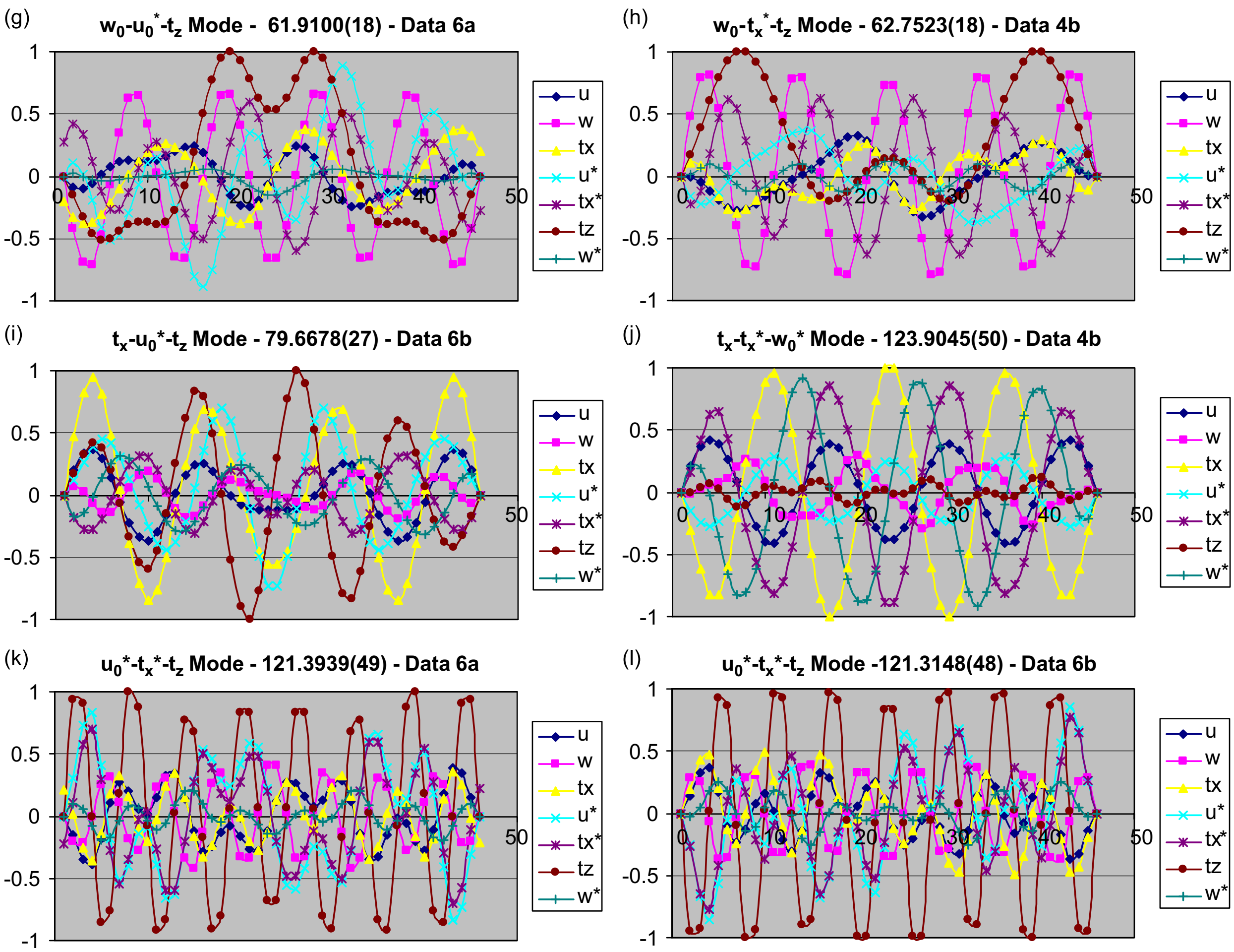

Fig. 9. (*Continued*)

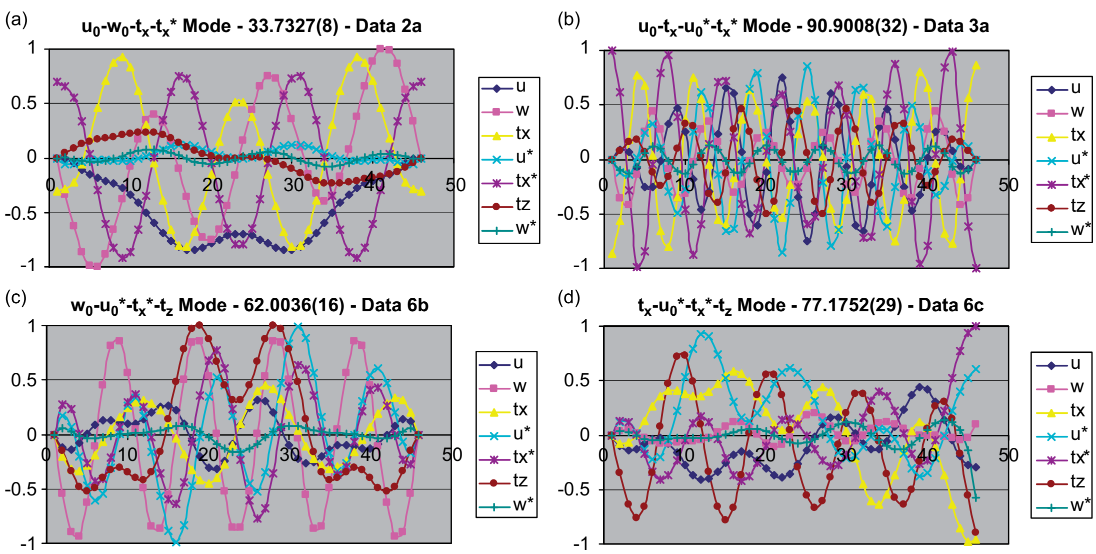

Fig. 10. (a)–(d) Quadruple dof coupled spectrum of thick circular arch.

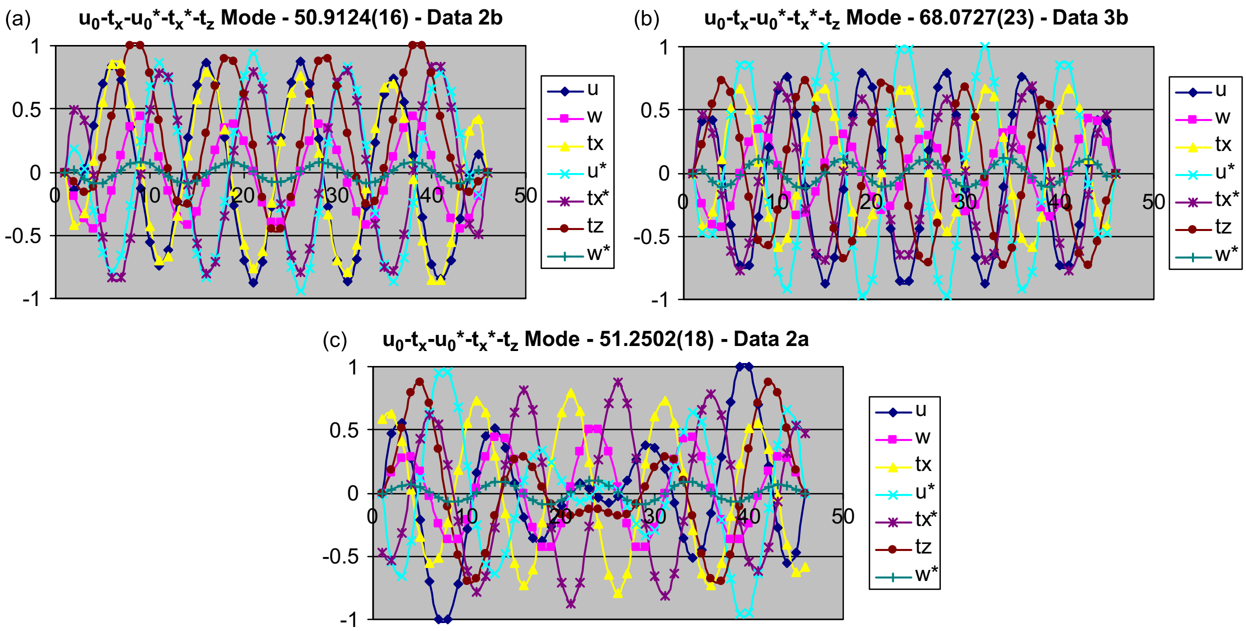

Fig. 11. (a)–(c) Quintuple dof coupled spectrum of thick circular arch.

Table 2
Comparison of frequency spectrums of a thin arch (Data-1)

Mode	Axial mode		Flexural mode		Shear mode	
	Ref. [11]	Present	Ref. [11]	Present	Ref. [11]	Present
1	119.6597	120.2329	8.4586	8.4647	3098.3860	3079.2039
2	331.1727	331.1710	37.5834	37.4993	3108.3938	3089.9311
3	546.7850	546.7877	84.8958	84.4452	3138.1073	3121.7062
4	763.1261	763.1325	151.3716	149.6671	3186.6435	3173.4939

Table 3
Frequency spectrum classification of SS-symmetric sandwich arch (Data-2a)

Mode	Frequency	Mode	Frequency	Mode	Frequency	Mode	Frequency
u	63.8312 (25)	$u-tz$	46.7847 (13)	$u-tx-u^*$	121.4699 (43)	$u-w-tx-tx^*$	30.6894 (7)
	91.4666 (34)	$tx-tx^*$	98.7302 (37)		147.6552 (49)		33.7327 (8)
w	8.2333 (1)		108.7471 (39)	$u-u^*-tz$	47.6499 (14)	$u-tx-u^*-tx^*$	61.0171 (23)
	11.7643 (2)		118.7401 (41)		47.6924 (15)		63.4014 (24)
	16.1545 (3)		129.3783 (45)		49.0255 (16)		67.2571 (26)
tx	16.921 (4)		140.4407 (48)		52.6033 (19)		70.9989 (28)
	33.9354 (9)			$w-tx-tx^*$	19.5958 (5)		73.7143 (29)
	69.3973 (27)				25.8831 (6)		78.6453 (30)
	97.1447 (36)				38.2832 (10)		80.9892 (31)
	125.4981 (44)				44.5227 (11)		86.4932 (32)
tz	46.7533 (12)						89.5069 (33)
	53.8026 (20)						94.7684 (35)
							102.5296 (38)
							111.201 (40)
							119.2038 (42)
							129.8557 (46)
							139.8085 (47)

Table 3 (*continued*)

Mode	Frequency	Mode	Frequency	Mode	Frequency	Mode	Frequency
							150.8811 (50)
						$u-tx-u^*-tx^*-tz$	49.4921 (17)
							51.2502 (18)
							56.4465 (21)
							57.0529 (22)

Note: The values given in parenthesis for each frequency correspond to the actual mode of arch vibration.

Table 4
Frequency spectrum classification of CC-symmetric sandwich arch (Data-2b)

Mode	Frequency	Mode	Frequency	Mode	Frequency	Mode	Frequency
w	8.9076 (1)	$u-tx$	84.7033 (31)	$u-tx-tx^*$	107.1955 (37)	$u-tx-u^*-tx^*$	65.6691 (24)
	12.5051 (2)		110.0602 (38)		135.4753 (45)		72.9785 (26)
	17.5047 (3)	$u-u^*$	87.1482 (32)		139.0875 (46)		73.3376 (27)
tx	28.6497 (6)		94.9933 (34)	$u-tx-tz$	44.8723 (10)		79.4739 (29)
	39.7238 (8)		102.743 (36)	$u-u^*-tz$	47.4963 (13)		129.7821 (43)
tz	47.071 (12)		111.5828 (40)		48.3151 (14)	$u-tx-u^*-tx^*-tz$	50.9124 (16)
	51.8513 (17)		120.8224 (41)		49.8322 (15)		52.4752 (18)
			140.1812 (47)		54.0493 (19)		56.8964 (20)
			150.8824 (49)	$w-tx-tx^*$	20.5785 (4)		58.6245 (21)
		$tx-tx^*$	75.2963 (28)		27.3025 (5)		59.5728 (22)
			82.6231 (30)		33.3263 (7)		62.6249 (23)
			91.7347 (33)		39.8545 (9)		67.305 (25)
			101.1061 (35)		46.3229 (11)		
			111.3756 (39)				
			121.5152 (42)				
			132.1602 (44)				
			143.2472 (48)				
			154.7411 (50)				

Note: The values given in parenthesis for each frequency correspond to the actual mode of arch vibration.

Table 5
Frequency spectrum classification of CF-symmetric sandwich arch (Data-2c)

Mode	Frequency	Mode	Frequency	Mode	Frequency	Mode	Frequency
w	5.02 (2)	$u-w$	2.0673 (1)	$u-tx-u^*$	71.5147 (29)	$u-tx-u^*-tx^*$	60.4403 (25)
	11.0439 (3)	$u-tx$	98.0457 (38)	$u-tx-tx^*$	123.7504 (45)		94.2601 (37)
	16.7315 (4)	$u-u^*$	56.6556 (23)	$u-u^*-tz$	46.1692 (12)		102.1708 (39)
tx	25.2719 (7)		61.5206 (26)		46.8772 (13)	$u-tx-u^*-tz$	47.2709 (14)
	38.579 (10)		66.9342 (27)		48.0548 (16)	$u-tx-u^*-tx^*-tz$	47.5216 (15)
	90.9158 (35)		73.9617 (30)		50.0588 (18)		54.2952 (22)
tz	48.6104 (17)		79.6826 (32)		51.5743 (19)		
	52.4708 (21)		87.1104 (34)		51.9884 (20)		
			111.279 (41)	$w-tx-tx^*$	23.6333 (6)		
			119.624 (43)		29.7774 (8)		
			129.8266 (47)		35.46 (9)		
			139.981 (49)		41.8642 (11)		
		$w-tx$	18.5482 (5)	$tx-u^*-tx^*$	103.0453 (40)		
		$tx-tx^*$	58.8709 (24)				
			67.185 (28)				
			75.2458 (31)				
			83.7298 (33)				
			92.8842 (36)				
			112.7165 (42)				
			122.3792 (44)				

Table 5 (*continued*)

Mode	Frequency	Mode	Frequency	Mode	Frequency	Mode	Frequency
			124.088 (46)				
			133.6584 (48)				
			144.5833 (50)				

Note: The values given in parenthesis for each frequency correspond to the actual mode of arch vibration.

Table 6
Frequency spectrum classification of SS-unsymmetric sandwich arch (Data-3a)

Mode	Frequency	Mode	Frequency	Mode	Frequency	Mode	Frequency
w	8.0723 (1)	$u-tx^{*}$	38.0586 (9)	$u-tx-u^{*}$	75.8359 (27)	$u-tx-u^{*}-tx^{*}$	66.1092 (23)
	12.7117 (2)	$w-tx^{*}$	19.2817 (5)	$u-tx-tx^{*}$	110.9231 (37)		72.6629 (26)
	17.5216 (4)	$tx-tx^{*}$	81.1935 (29)		147.2326 (46)		90.9008 (32)
tx	16.9147 (3)		144.2245 (45)	$u-u^{*}-tx^{*}$	72.0279 (25)		94.7261 (33)
	38.338 (10)		152.5856 (48)		79.5389 (28)		109.6503 (36)
	83.2577 (30)		156.9655 (49)		86.7917 (31)		112.2467 (38)
	117.8687 (39)	$tx-tz$	57.3092 (20)		102.851 (35)		119.4814 (40)
tz	48.6814 (12)	$u^{*}-tz$	49.8995 (14)		129.2973 (42)		
	49.0917 (13)				139.19 (44)		
					149.9731 (47)		
					161.3683 (50)		
				$u-u^{*}-tz$	50.4877 (15)		
					52.0268 (17)		
					54.1556 (18)		
					56.8099 (19)		
					60.7757 (22)		
					66.4285 (24)		
				$w-tx-tx^{*}$	25.2751 (6)		
					31.4357 (7)		
					38.0227 (8)		
					45.0083 (11)		
					51.9557 (16)		
				$tx-u^{*}-tx^{*}$	59.4767 (21)		
					99.9419 (34)		
					122.6996 (41)		
					132.9441 (43)		

Note: The values given in parenthesis for each frequency correspond to the actual mode of arch vibration.

Table 7
Frequency spectrum classification of CC-unsymmetric sandwich arch (Data-3b)

Mode	Frequency	Mode	Frequency	Mode	Frequency	Mode	Frequency
w	8.6691 (1)	$u-tx$	71.5314 (24)	$u-tx-tx^{*}$	132.7422 (41)	$u-tx-u^{*}-tx^{*}$	84.237 (28)
	13.0454 (2)		135.7116 (43)	$u-u^{*}-tx^{*}$	79.8305 (27)		93.8829 (31)
	19.7133 (3)		168.1807 (49)		86.8099 (29)		94.9289 (32)
tx	35.0035 (7)	$u-u^{*}$	111.1716 (36)		120.2945 (38)		101.8846 (33)
tz	48.1157 (10)		161.6149 (48)		129.7457 (40)		103.856 (35)
	49.4537 (12)	$w-tx^{*}$	20.1804 (4)		139.8861 (44)	$u-tx-u^{*}-tx^{*}-tz$	66.3445 (22)
	52.827 (15)	$tx-tx^{*}$	45.2945 (9)		150.5046 (46)		68.0727 (23)
			91.4357 (30)	$u-u^{*}-tz$	51.5562 (14)		73.0073 (25)
			103.344 (34)		54.6405 (17)		75.4708 (26)
			114.0134 (37)		55.6449 (18)		
			124.4052 (39)		58.5805 (19)		

Table 7 (*continued*)

Mode	Frequency	Mode	Frequency	Mode	Frequency	Mode	Frequency
			135.4948 (42)		61.7422 (21)		
			146.9745 (45)	$w-tx-tx^*$	27.1209 (5)		
			158.8316 (47)		32.3097 (6)		
			171.1862 (50)		39.9119 (8)		
		u^*-tz	50.2463 (13)		48.1301 (11)		
					53.7811 (16)		
				$tx-u^*-tx^*$	60.5821 (20)		

Note: The values given in parenthesis for each frequency correspond to the actual mode of arch vibration.

Table 8
Frequency spectrum classification of CF-unsymmetric sandwich arch (Data-3c)

Mode	Frequency	Mode	Frequency	Mode	Frequency	Mode	Frequency
w	5.0112 (2)	$u-w$	2.1102 (1)	$u-tx-tx^*$	112.8042 (39)	$u-tx-u^*-tx^*$	87.8285 (33)
	10.8886 (3)	$w-tx$	20.6184 (5)		152.7827 (50)	$u-tx-u^*-tx^*-tz$	62.4453 (24)
	16.4168 (4)	$tx-tx^*$	72.0568 (27)	$u-u^*-tz$	57.0893 (21)		68.884 (26)
tx	119.4977 (41)		85.4792 (31)		58.4373 (22)		
	152.1115 (49)		95.0092 (35)	$w-tx-tx^*$	23.9336 (6)		
u^*	60.7335 (23)		104.6138 (37)		27.4785 (7)		
	66.7095 (25)		115.2747 (40)		31.0933 (8)		
	73.0936 (28)		125.9907 (43)		35.1856 (9)		
	79.7142 (30)		136.9176 (45)		41.6295 (10)		
	86.1427 (32)		148.3366 (47)	$tx-u^*-tx^*$	76.9725 (29)		
	94.5551 (34)	$tx-tz$	44.543 (11)				
	102.6411 (36)	u^*-tz	48.7671 (13)				
	111.1374 (38)		50.2098 (16)				
	120.3573 (42)		51.4694 (17)				
	129.9527 (44)		53.2411 (18)				
	139.9263 (46)		54.4035 (19)				
	150.5249 (48)						
tx^*	55.148 (20)						
tz	47.9062 (12)						
	49.4266 (14)						
	49.4749 (15)						

Note: The values given in parenthesis for each frequency correspond to the actual mode of arch vibration.

Table 9
Frequency spectrum classification of SS-symmetric composite arch (Data-4a)

Mode	Frequency	Mode	Frequency	Mode	Frequency
u	17.1268 (4)	$u-w$	7.6069 (2)	$u-w-tx$	32.6636 (7)
w	7.1423 (1)		30.6784 (6)	$tx-u^*-tz$	63.4756 (21)
	15.6589 (3)	$w-tx^*$	46.8214 (12)		114.7298 (46)
	23.5601 (5)		54.6435 (14)		
	38.9768 (9)		62.3818 (19)		
tx	38.6591 (8)		70.2225 (24)		
	42.7611 (10)		78.0706 (28)		
	46.3039 (11)		85.9466 (31)		
	53.0333 (13)		93.8187 (35)		
	68.0955 (23)		110.0487 (44)		
	74.4081 (26)		117.8106 (48)		

Table 9 (*continued*)

Mode	Frequency	Mode	Frequency	Mode	Frequency
	83.2902 (30)	$tx-tx^*$	101.3673 (39)		
	87.8175 (33)		101.9185 (40)		
	98.6191 (37)	$tx-tz$	57.4568 (15)		
	113.7812 (45)	u^*-tz	93.5273 (34)		
	114.744 (47)		100.1575 (38)		
u^*	96.7479 (36)		107.1918 (42)		
	102.2324 (41)		122.2933 (50)		
	109.6089 (43)				
	119.0127 (49)				
tz	60.4925 (16)				
	60.5638 (17)				
	61.484 (18)				
	62.8713 (20)				
	66.8592 (22)				
	71.3381 (25)				
	75.9149 (27)				
	81.3911 (29)				
	87.3601 (32)				

Note: The values given in parenthesis for each frequency correspond to the actual mode of arch vibration.

Table 10
Frequency spectrum classification of CC-symmetric composite arch (Data-4b)

Mode	Frequency	Mode	Frequency	Mode	Frequency
w	8.1407 (1)	$u-w$	9.345 (2)	$u-w-tx$	32.8628 (7)
	17.279 (3)		17.3362 (4)	$w-tx-tx^*$	39.2795 (8)
	24.6143 (5)		31.1221 (6)		77.6891 (26)
tx	42.8488 (9)	$u-tx$	46.7364 (10)	$w-tx^*-tz$	62.7523 (18)
	52.4904 (12)	$w-tx^*$	46.9731 (11)	$tx-u^*-tz$	77.7276 (27)
	65.1991 (21)		54.8899 (13)	$tx-tx^*-w^*$	123.9045 (50)
	91.3163 (32)		70.7664 (23)		
	94.6417 (35)		86.0923 (30)		
	105.3591 (40)		94.0694 (34)		
	118.7238 (47)		102.0296 (38)		
u^*	96.7634 (36)		117.8952 (46)		
	102.0925 (39)	$tx-tx^*$	80.22 (28)		
	109.8232 (43)		109.1915 (42)		
	119.0437 (48)		110.8979 (44)		
tz	58.3909 (14)	u^*-tz	93.6344 (33)		
	60.3368 (15)		100.1957 (37)		
	60.5813 (16)		107.1703 (41)		
	61.4218 (17)		114.4496 (45)		
	62.9386 (19)		122.382 (49)		
	65.1057 (20)				
	66.9844 (22)				
	71.2089 (24)				
	75.6067 (25)				
	81.3923 (29)				
	87.3257 (31)				

Note: The values given in parenthesis for each frequency correspond to the actual mode of arch vibration.

Table 11
Frequency spectrum classification of CF-symmetric composite arch (Data-4c)

Mode	Frequency	Mode	Frequency	Mode	Frequency
u	24.7492 (6)	*u*–*w*	1.0428 (1)	*u*–*tx*–*tz*	53.3815 (14)
w	4.0043 (2)		9.2245 (3)	*w*–*tx*–*tx**	50.4255 (13)
	12.5771 (4)	*u*–*tx*	39.2658 (9)	*tx*–*u**–*tz*	70.4415 (25)
	18.3858 (5)	*w*–*tx*	33.3268 (8)		71.7234 (27)
	26.0905 (7)	*tx*–*tx**	74.9414 (28)	*tx*–*tx**–*tz*	59.0044 (17)
tx	39.824 (10)		98.5586 (39)		
	42.4521 (11)		116.8545 (49)		
	47.503 (12)	*tx*–*tz*	57.632 (16)		
	71.0653 (26)	*u**–*tz*	76.3986 (29)		
	84.4582 (32)		81.9698 (31)		
	87.1763 (33)		87.8975 (34)		
	101.8519 (41)		93.7676 (36)		
	112.087 (46)		119.15 (50)		
*u**	97.0322 (38)				
	99.3898 (40)				
	103.2582 (42)				
	106.0743 (44)				
	110.8764 (45)				
	113.755 (48)				
*tx**	66.3678 (23)				
	81.1596 (30)				
	89.3796 (35)				
	96.9329 (37)				
	104.9344 (43)				
	112.5024 (47)				
tz	56.2543 (15)				
	60.2704 (18)				
	60.6832 (19)				
	61.0543 (20)				
	61.3552 (21)				
	63.3299 (22)				
	66.7752 (24)				

Note: The values given in parenthesis for each frequency correspond to the actual mode of arch vibration.

Table 12
Frequency spectrum classification of SS-unsymmetric composite arch (Data-6a)

Mode	Frequency	Mode	Frequency	Mode	Frequency	Mode	Frequency
w	6.8674 (1)	*u*–*u**	88.6634 (33)	*w*–*u**–*tx**	54.4248 (13)	*w*–*u**–*tx**–*tz*	76.7004 (27)
	9.2117 (2)	*u*–*tx*	15.9204 (3)		69.2109 (24)		91.5372 (34)
	16.9621 (4)		29.3914 (6)		83.9298 (30)		106.6657 (42)
	24.7053 (5)	*w*–*tx*	40.0544 (10)	*w*–*u**–*tz*	61.91 (18)		
	32.3763 (7)		46.6899 (11)	*tx*–*u**–*tx**	116.1363 (47)		
tx	38.1678 (8)	*tx*–*u**	88.2008 (32)	*tx*–*u**–*tz*	73.5612 (25)		
	39.0395 (9)	*tx*–*tx**	47.8561 (12)		78.7935 (28)		
*u**	97.4908 (36)	*tx*–*tz*	55.7888 (14)		109.0035 (43)		
	98.1252 (37)		56.6081 (15)	*u**–*tx**–*tz*	121.3939 (49)		
	100.3696 (39)		67.8004 (22)		121.9506 (50)		
	101.3436 (40)		68.7754 (23)				
	112.4932 (44)	*u**–*tx**	113.1618 (45)				
	118.6444 (48)	*u**–*tz*	86.5506 (31)				
tz	60.8305 (16)		100.1539 (38)				
	61.2141 (17)		106.2195 (41)				
	63.4701 (19)						

Table 12 (*continued*)

Mode	Frequency	Mode	Frequency	Mode	Frequency	Mode	Frequency
	63.7428 (20)						
	67.7578 (21)						
	75.3674 (26)						
	81.461 (29)						
	93.6994 (35)						
	113.9282 (46)						

Note: The values given in parenthesis for each frequency correspond to the actual mode of arch vibration.

Table 13
Frequency spectrum classification of CC-unsymmetric composite arch (Data-6b)

Mode	Frequency	Mode	Frequency	Mode	Frequency	Mode	Frequency
w	10.4302 (1)	u−tx	20.8867 (4)	w−tx−tx*	46.7716 (10)	w−tx−u*−tx*	54.0099 (12)
	13.1888 (2)		29.6713 (6)	w−u*−tx*	76.6412 (26)	w−u*−tx*−tz	62.0036 (16)
	19.7022 (3)	w−tx	40.2042 (9)		91.794 (33)		69.4396 (23)
	25.3527 (5)	tx−u*	97.5011 (35)	tx−u*−tz	75.4997 (25)		84.1589 (29)
	32.7974 (7)	tx−tx*	48.4371 (11)		79.6678 (27)	tx−u*−tx*−tz	106.1732 (40)
tx	38.3732 (8)	tx−tz	68.8038 (22)	u*−tx*−tz	106.5977 (41)		
	56.1813 (13)		88.417 (32)		121.3148 (48)		
	57.4607 (14)		108.5703 (42)				
u*	84.4956 (30)	tx−w*	117.8186 (46)				
	98.1179 (36)		127.281 (50)				
	100.0795 (37)	u*−tx*	114.1159 (45)				
	104.4142 (39)		119.7185 (47)				
	110.5366 (43)		122.0714 (49)				
tz	61.0808 (15)	u*−tz	62.5713 (17)				
	63.4523 (18)		66.119 (20)				
	64.2741 (19)		87.4574 (31)				
	68.4255 (21)		100.5913 (38)				
	72.9479 (24)						
	81.4702 (28)						
	93.8192 (34)						
	113.9239 (44)						

Note: The values given in parenthesis for each frequency correspond to the actual mode of arch vibration.

Table 14
Frequency spectrum classification of CF-unsymmetric composite arch (Data-6c)

Mode	Frequency	Mode	Frequency	Mode	Frequency	Mode	Frequency
w	4.8024 (2)	u−w	1.1606 (1)	tx−u*−tz	83.8623 (32)	tx−u*−tx*−tz	72.1729 (26)
	10.7323 (3)	w−tx	18.0372 (4)		92.7984 (36)		77.1752 (29)
	28.4065 (7)		19.203 (5)		101.9568 (41)		104.2277 (42)
tx	25.2757 (6)	u*−tx*	86.4852 (33)	w−tx−u*	40.9808 (10)		
	32.9387 (8)		99.9229 (40)	u*−tx*−tz	79.4408 (30)		
	36.0093 (9)		108.0026 (44)		96.0051 (38)		
	43.8313 (11)		113.9778 (47)		117.1148 (49)		
	45.3679 (12)		115.6319 (48)	tx−u*−w*	113.1272 (46)		
	53.0256 (14)		119.1571 (50)				
u*	92.0238 (35)	tx−u*	76.1183 (28)				
	94.3852 (37)	tx−tz	49.8517 (13)				
	99.3515 (39)	u*−tz	55.2855 (15)				
	106.4655 (43)		60.8178 (18)				

Table 14 (*continued*)

Mode	Frequency	Mode	Frequency	Mode	Frequency	Mode	Frequency
tz	58.856 (16)		62.4568 (20)				
	60.3345 (17)		65.3898 (22)				
	61.4731 (19)		68.019 (24)				
	64.1318 (21)		70.7826 (25)				
	66.5262 (23)		74.9209 (27)				
			82.3844 (31)				
			88.9037 (34)				
			109.9825 (45)				

Note: The values given in parenthesis for each frequency correspond to the actual mode of arch vibration.

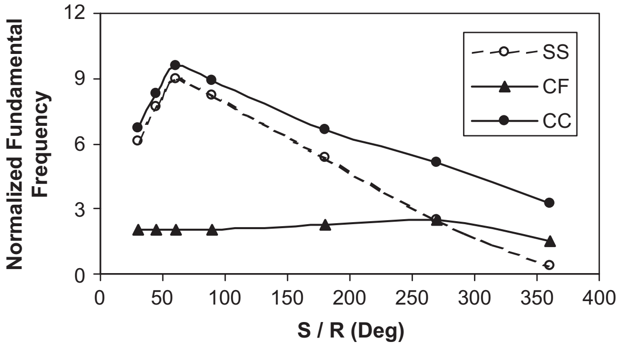

Fig. 12. Effect of curvature: symmetric sandwich (Data-2)—$S/t = 5$.

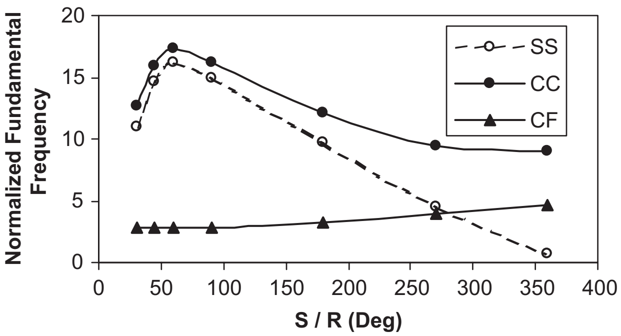

Fig. 13. Effect of curvature: symmetric sandwich (Data-2)—$S/t = 10$.

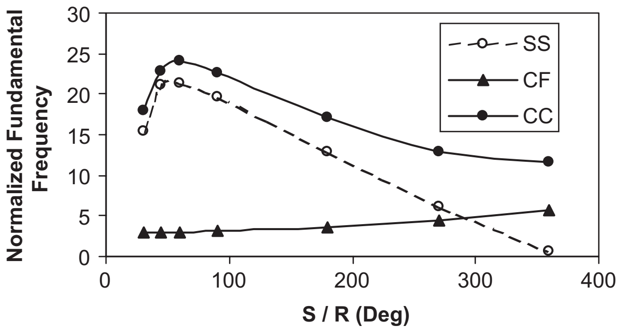

Fig. 14. Effect of curvature: symmetric sandwich (Data-2)—$S/t = 15$.

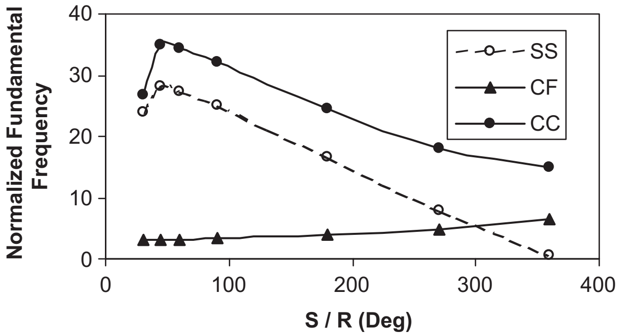

Fig. 15. Effect of curvature: symmetric sandwich (Data-2)—$S/t = 25$.

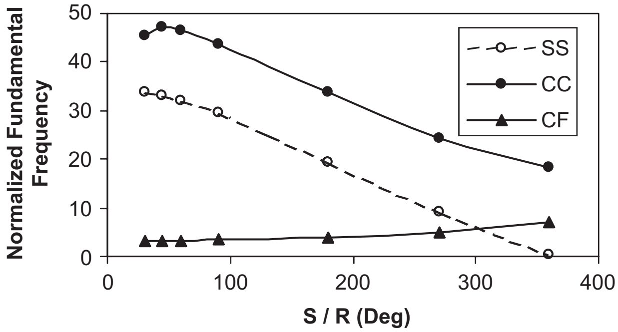

Fig. 16. Effect of curvature: symmetric sandwich (Data-2)—$S/t = 50$.

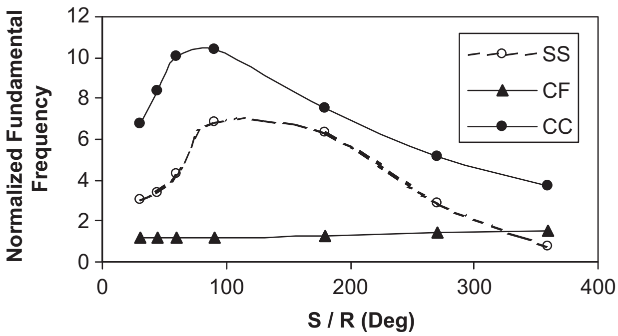

Fig. 17. Effect of curvature: unsymmetric composite (Data-6)—$S/t = 5$.

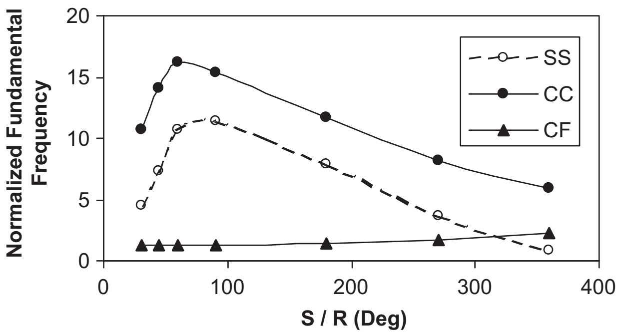

Fig. 18. Effect of curvature: unsymmetric composite (Data-6)—$S/t = 10$.

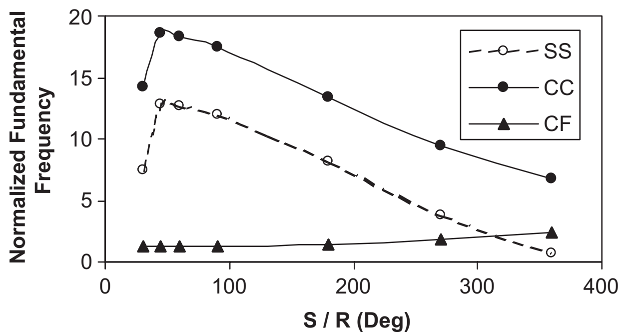

Fig. 19. Effect of curvature: unsymmetric composite (Data-6)—$S/t = 15$.

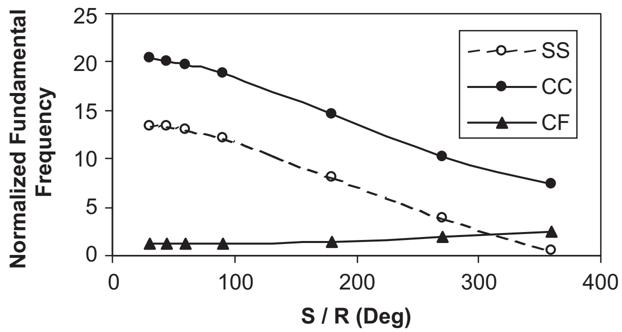

Fig. 20. Effect of curvature: unsymmetric composite (Data-6)—$S/t = 25$.

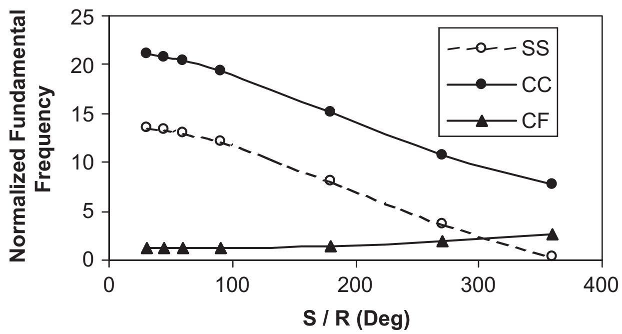

Fig. 21. Effect of curvature: unsymmetric composite (Data-6)—$S/t = 50$.

The future scope of this work would be to extend the current theory to elliptical arches with varying cross sections.

Acknowledgements

The first author gratefully acknowledges the useful suggestions regarding frequency spectra analysis, given by Dr. Gangan Prathap of CMMACS, CSIR, Bangalore, during the preparation of this manuscript.

References

[1] J.A. Wolf Jr., Natural frequencies of circular arches, *ASCE Journal of Structural Division* 97 (1971) 2337–2350.

[2] A.S. Veletsos, W.J. Austin, C.A.L. Pereira, S.J. Wung, Free in plane vibration of circular arches, *ASCE Journal of Engineering Mechanics Division* 98 (1972) 311–329.

[3] W.J. Austin, A.S. Veletsos, Free vibration of arches flexible in shear, *ASCE Journal of Engineering Mechanics Division* 99 (1973) 735–753.

[4] G.R. Bhashyam, G. Prathap, The second frequency spectrum of Timoshenko beams, *Journal of Sound and Vibration* 76 (1981) 407–420.

[5] G.R. Heppler, An element for studying the vibration of unrestrained curved Timoshenko beams, *Journal of Sound and Vibration* 158 (1992) 387–404.

[6] T. Sakiyama, H. Matsuda, C. Morita, Free vibration analysis of sandwich arches with elastic or visco elastic core and various kinds of axis shape and boundary conditions, *Journal of Sound and Vibration* 203 (1997) 505–522.

[7] G. Prathap, R.U. Vinayak, Vibrations of laminated beams using higher order theory, *Advanced Composite Materials* 6 (1996) 33–50.

[8] R.D. Blevins, *Formulas for Natural Frequency and Mode Shape*, Krieger Publishing Company, Florida, 2001.

[9] S.P. Timoshenko, On the correction for shear in differential equation for transverse vibrations of prismatic bars, *Philosophical Magazine Series* 41 (1921) 744–746.

[10] G.R. Cowper, The shear coefficient in Timoshenko beam theory, *ASME Journal of Applied Mechanics* 33 (1966) 335–340.

[11] P. Jafarali, S. Mukherjee, G. Prathap, Free vibration analysis of curved beams. Annual Report, CSIR Center for Mathematical Modeling and Computer Simulation, Bangalore, 2004.

[12] J.K. Chen, C.T. Sun, Nonlinear transient responses of initially stressed composite plates, *Computers and Structures* 21 (1985) 513–520.

[13] H.G. Allen, *Analysis and Design of Structural Sandwich Panels*, Pergamon Press, London, 1969.

[14] J.N. Reddy, On the solutions to forced motions of rectangular composite plates, *ASME Journal of Applied Mechanics* 49 (1982) 403–408.

[15] S.R. Marur, T. Kant, Free vibration analysis of fiber reinforced composite beams using higher order theories and finite element modeling, *Journal of Sound and Vibration* 194 (1996) 337–351.

[16] S.R. Marur, T. Kant, A higher order finite element model for the vibration analysis of laminated beams, *ASME Journal of Vibration and Acoustics* 120 (1998) 822–824.

[17] S.R. Marur, T. Kant, Free vibration of higher-order sandwich and composite arches, part I: formulation, *Journal of Sound and Vibration*, in press, doi:10.1016/j.jsv.2007.07.084.